

## FORMULATION DESIGN AND OPTIMISATION OF SUSTAINED RELEASE HYDROPHILIC MATRIX TABLET OF SORAFENIB USING FACTORIAL DESIGN

SHAWKAT ISLAM<sup>1</sup>, ABU SHARA SHAMSUR ROUF<sup>2</sup> AND OMAR FARUK<sup>1\*</sup>

<sup>1</sup>Department of Pharmacy, Faculty of Sciences and Engineering,  
East West University, Dhaka-1212, Bangladesh

<sup>2</sup>Department of Pharmaceutical Technology, Faculty of Pharmacy,  
University of Dhaka, Dhaka-1000, Bangladesh

**Published online:** 28 November 2025

**To cite this article:** ISLAM, S., ROUF, A. S. S. & FARUK, O. (2025) Formulation design and optimisation of sustained release hydrophilic matrix tablet of sorafenib using factorial design, *Malaysian Journal of Pharmaceutical Sciences*, 23(2): 1–20. <https://doi.org/10.21315/mjps2025.23.2.1>

**To link to this article:** <https://doi.org/10.21315/mjps2025.23.2.1>

### ABSTRACT

*Sorafenib (SFB), a multi-kinase inhibitor used in the treatment of certain cancers, is typically administered as two 200 mg tablets twice daily, which can result in variable plasma levels and reduced patient compliance. This study aimed to develop a 400 mg sustained release hydrophilic matrix tablet of SFB, using factorial design to optimise drug release profiles. Hydroxypropyl methylcellulose (HPMC) was utilised as the primary matrix forming agent, with additional excipients selected based on compatibility studies. Employing a 3<sup>2</sup> full factorial design, the study optimised key formulation variables, specifically the concentrations of HPMC and Povidone K30, to achieve the desired release characteristics. Nine prototype formulations were evaluated for drug release at specified intervals (2, 8 and 12 hours). An optimal formulation was identified through statistical and empirical analysis, requiring 6.05% Methocel® K15M and 4.39% Povidone K30. The optimised formulation demonstrated release kinetics consistent with the Higuchi model, indicating sustained drug release with a high R<sup>2</sup> value (0.9999). The findings from this study suggested a novel tablet dosage form for SFB, allowing patients to take a single tablet instead of two at a time, thus simplifying the dosing schedule and maintaining stable therapeutic plasma levels.*

**Keywords:** Sorafenib, Sustained release formulation, Hydrophilic matrix tablet, Factorial design, Quality by design (QbD)

### INTRODUCTION

Sorafenib (SFB) is a multi-kinase inhibitor widely used for treating certain types of cancer, including advanced renal cell carcinoma (RCC) and hepatocellular carcinoma (HCC) (Llovet *et al.* 2008; Man *et al.* 2021). It suppresses tumour cell growth and angiogenesis while

---

\*Corresponding author: [omar.faruk@ewubd.edu](mailto:omar.faruk@ewubd.edu)

promoting apoptosis across various tumour models (Tang *et al.* 2020; Kong *et al.* 2021). It works by inhibiting the serine-threonine kinases Raf-1 and B-Raf, as well as the receptor tyrosine kinase activities of vascular endothelial growth factor receptors (VEGFRs) 1, 2 and 3, along with platelet-derived growth factor receptor  $\beta$  (PDGFR- $\beta$ ) (Abdu *et al.* 2022; Cheng *et al.* 2022; Li *et al.* 2023). Chemically, SFB is known as 4-(4-(3-(4-chloro-3-(trifluoromethyl)phenyl)ureido)phenoxy)-N-methylpicolinamide (Aman *et al.* 2023).

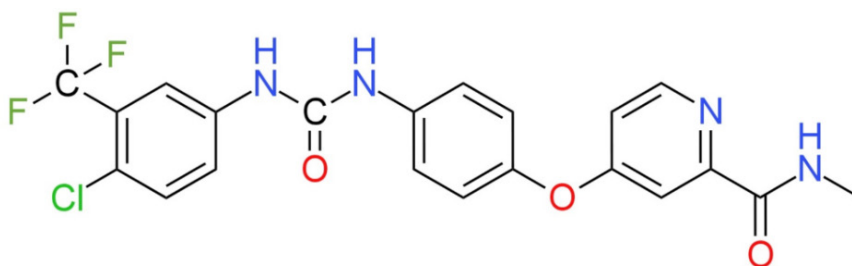


**Figure 1:** 2D chemical structure of sorafenib.

SFB is typically administered as two 200 mg tablets twice daily, providing a total dose of 800 mg daily (Alghamdi *et al.* 2020; Tak *et al.* 2020). This regimen however, can lead to fluctuations in plasma drug concentrations and may be inconvenient for patients, potentially affecting compliance and therapeutic efficacy (Pang *et al.* 2022).

Sustained-release drug formulations (SRDF) have been explored as a strategy to achieve prolonged therapeutic effects by maintaining a stable drug-release profile over an extended period (Chaudhari *et al.* 2012). SRDFs are designed to release the drug slowly and consistently, enhancing bioavailability while reducing dosing frequency (Mamidala *et al.* 2009; Kamboj *et al.* 2012; Darandale *et al.* 2017). Hydrophilic polymers, particularly hydroxypropyl methylcellulose (HPMC), are commonly used in SRDFs due to their matrix-forming ability, which effectively controls drug release rates (Wu and Jin 2008). HPMC matrices form a gel barrier upon hydration, which allows for gradual drug diffusion, making them an ideal choice for formulating hydrophilic matrix-based SR tablets (Pundir *et al.* 2013; Goyal *et al.* 2017).

For optimising such formulations, the quality by design (QbD) approach is instrumental in systematically studying the effects of formulation and process variables on drug release characteristics (Goldfarb 2006; Yu *et al.* 2014; Kolekar 2019). Factorial design, a subset of QbD, allows for the simultaneous evaluation of multiple factors and their interactions, thus enhancing the efficiency of the formulation development process (Hwang and Noack 2011; Politis *et al.* 2017; Kovács *et al.* 2021). By applying a full factorial design, researchers can identify the optimal combination of excipients, polymer concentrations, and other critical formulation factors that contribute to the desired sustained-release profile (Nandi *et al.* 2022).

This study aimed to develop a 400 mg sustained-release tablet of SFB, which will gradually release SFB over a 12 hour period, allowing patients to take a single tablet rather than two, simplifying the dosage schedule while maintaining stable therapeutic plasma levels.

## MATERIALS

SFB (potency = 99.8%) was generously gifted by Eskayef Pharmaceuticals Limited, Bangladesh. Hydroxypropyl methylcellulose (Methocel® K15M CR, Colorcon, India), microcrystalline cellulose (Avicel PH 101, Mingtai Chemical Co. Ltd., China), dibasic calcium phosphate (Qualikems Fine Chem Pvt. Ltd., India), Povidone K30 (Sisco Research Lab Pvt. Ltd., India), magnesium stearate (Loba Chemie Pvt. Ltd., India), and talc (Merck KGaA, Germany) were purchased from the local market.

## METHODS

### Excipient Selection

The excipients were selected after a critical review of literatures and performing drug-excipient compatibility studies. Compatibility between the active pharmaceutical ingredient (API) and excipients was evaluated using fourier transform infrared spectroscopy (FTIR).

### Preliminary Screening

Preliminary studies involved preparing SFB formulations with Methocel® K15M CR and Povidone K30 at various ratios. The physicochemical properties and dissolution profiles of the formulations were assessed following standard protocols. Based on the observed dissolution rates, the upper and lower concentration limits of these excipients were determined for further analysis. Table 1 presents the overall excipient ranges used in the formulation of the SFB SR tablet.

**Table 1:** Composition of SFB sustained-release matrices during preliminary studies.

Name of the ingredients	Justification of use	Amount (%)	Amount (mg)
SFB	Active pharmaceutical ingredient	72.73	400
Methocel® K15M CR	Release retardant	2–12	11–66
Povidone K30	Binder	1–6	5.5–33.0
Avicel PH 101	Diluent	4.36–13.36	24.0–73.5
Dibasic calcium phosphate	Diluent	2.90–8.90	16–49
Purified talc	Glidant	1.2	6.6
Magnesium stearate	Lubricant	0.8	4.4

### Tablet Preparation

The active ingredient, polymers, filler, glidant and lubricant were accurately weighed and sieved through a no. 40 mesh (425 µm diameter). The active ingredient and excipients (excluding half of the talc and magnesium stearate) were then blended in a v-blender (VB-50, GlobePharma Inc., USA) for approximately 10 minutes. Isopropyl alcohol was added to create a dough-like mass, which was subsequently passed through a no. 30 mesh (600 µm diameter) sieve. The resulting wet granules were dried in a tray dryer (TD-24, Labtop

Instruments Pvt. Ltd., India) for 50 minutes. After drying, the remaining talc and magnesium stearate were incorporated into the granules and thoroughly mixed. The prepared granules were then compressed on a rotary tablet press (Fette 2090i, Fette Compacting GmbH, Germany) at a compression force of 2 tonnes.

### Evaluation of Flow Characteristics

The flow characteristics of the prepared SFB granules were evaluated based on parameters such as the Hausner ratio, Carr's index and angle of repose.

#### Determination of bulk density

Bulk density was measured by pouring pre-weighted granules into a 10 mL measuring cylinder and the volume was noted. Then it was calculated according to equation 1.

$$\text{Bulk density, } D_b = \frac{w}{V_b} \quad (\text{Equation 1})$$

where,  $w$  = weight of granules and  $V_b$  = bulk volume.

#### Determination of tapped density

After measuring the bulk density, the granules were tapped 500 times by tapped density tester (Electrolab, New Delhi, India) and the volume was measured. This volume was considered as the tapped volume. Tapped density was calculated according to Equation 2.

$$\text{Tapped density, } D_t = \frac{w}{V_t} \quad (\text{Equation 2})$$

where,  $w$  = weight of granules and  $V_t$  = tapped volume.

#### Hausner ratio

The Hausner ratio is used to assess the flowability of granules by comparing the tapped density and bulk density. The Hausner ratio was calculated using the following equation.

$$\text{Hausner ratio} = \frac{D_t}{D_b} \quad (\text{Equation 3})$$

where,  $D_t$  = tapped density and  $D_b$  = bulk density.

#### Carr's index

The Carr's index measures the compressibility of granules, indicating how well it will flow under pressure. The equation provided below was used to measure Carr's index.

$$\text{Carr's index} = \frac{D_t - D_b}{D_t} \times 100\% \quad (\text{Equation 4})$$

### Angle of repose

The angle of repose ( $\theta$ ) is used to assess the flowability of granules by measuring the maximum angle between the surface of a pile of granules and the horizontal plane. It was determined using the fixed funnel method. In this method, the granules were poured through a funnel, which was gradually raised vertically until the maximum cone height ( $h$ ) was achieved. The radius of the base of the cone ( $r$ ) was then carefully measured. The angle of repose was calculated using the following equation.

$$\text{Angle of repose, } \theta = \tan^{-1} \frac{h}{r} \quad (\text{Equation 5})$$

### Evaluation of tablet Properties

#### Tablet length, width and thickness determination

The measurements were performed by placing tablets between the two arms of the Vernier callipers. Six tablets from each batch were measured for each parameter.

#### Weight variation test

Individual weights of 10 tablets from each batch were weighed accurately using an electronic balance (AY220, Shimadzu, Japan) to calculate the uniformity of weight. It was calculated using the following equation.

$$\text{Weight variation} = \frac{I_w - A_w}{A_w} \times 100\% \quad (\text{Equation 6})$$

where,  $I_w$  = individual weight of tablet and  $A_w$  = average weight of tablets.

#### Hardness test

The hardness of six tablets from each batch was determined by calculating the force required to crush the tablets using an automatic tablet hardness tester (Unitech, New Delhi, India).

#### Friability test

The Roche friabilator (Electrolab, New Delhi, India) was used for this test. Ten tablets from each batch were weighed accurately and placed in the tumbling apparatus, which revolved at 25 rpm, causing the tablets to drop from a height of six inches with each revolution. After 4 minutes, the tablets were weighed again, and the percentage loss in tablet weight was determined. Friability was then calculated using the following equation.

$$\%Friability = \frac{W_i - W_f}{W_i} \times 100\%$$

(Equation 7)

where  $W_i$  = initial weight of tablets and  $W_f$  = final weight of tablets.

Dissolution Studies

The in vitro dissolution studies were performed in 900 mL of pH 6.8 phosphate buffer over a 12 hour period using a United States Pharmacopeia (USP) type II (paddle) dissolution apparatus (DIS 8000, Electrolab, India) maintained at a temperature of  $37 \pm 0.5^\circ\text{C}$  with a paddle rotation speed of 50 rpm.

Experimental Design and Formulation Optimisation

A  $3^2$  full factorial design was created using Design Expert® software (V. 13, Stat-Ease Inc., Minneapolis, USA) as outlined in Table 2. The percentages of Povidone K30 and Methocel® K15M CR were treated as covariates, while the drug release percentages at pH 6.8 phosphate buffer after 2, 8 and 12 hours served as the dependent variables. The experimental design included low, medium and high levels for each covariate, resulting in nine prototype formulations suggested for further investigation, as shown in Table 3.

Table 2: Variables and responses for experimental design.

Variables	Levels used actual (coded)		
	Low (−1)	Mid (0)	High (+1)
A = Methocel® K15M CR	5	7.5	10
B = Povidone K30	1	2.5	5
Responses	Constraints		
$Q_2$ = Cumulative % drug release after 2 h	$0\% \leq Q_2 \leq 25\%$		
$Q_8$ = Cumulative % drug release after 8 h	$50\% \leq Q_8 \leq 75\%$		
$Q_{12}$ = Cumulative % drug release after 12 h	$80\% \leq Q_{12} \leq 100\%$		

Table 3: Formulation of nine different (F1 to F9) tablet batches (mg/tablet).

Batch	SFB	Povidone K30	Methocel® K15M CR	Avicel PH 101	Dibasic calcium phosphate	Talc	Mg stearate	Total
F1	400	27.50	27.50	56.00	28.00	6.6	4.4	550
F2	400	5.50	55.00	52.33	26.17	6.6	4.4	550
F3	400	27.50	41.25	46.83	23.42	6.6	4.4	550
F4	400	13.75	55.00	46.83	23.42	6.6	4.4	550
F5	400	13.75	27.50	65.17	32.58	6.6	4.4	550
F6	400	13.75	41.25	56.00	28.00	6.6	4.4	550
F7	400	5.50	41.25	61.50	30.75	6.6	4.4	550
F8	400	5.50	27.50	70.67	35.33	6.6	4.4	550
F9	400	27.50	55.00	37.67	18.83	6.6	4.4	550

## Drug Release Kinetics Studies

The in vitro release kinetics of the optimised tablet batch were evaluated using zero-order, first-order, Hixson-Crowell, Higuchi and Korsmeyer-Peppas models.

### Zero-order release kinetics

Zero-order release indicates a constant drug release rate, independent of concentration. The drug is released in a constant amount over time.

$$C = K_0 t \quad (\text{Equation 8})$$

where,  $C$  = drug concentration at time,  $K_0$  = zero order rate constant,  $t$  = time in hour.

### First-order release kinetics

First-order release implies that the rate of drug release is proportional to the remaining amount of drug in the system. The drug is released in a decaying manner over time.

$$C = C_0 e^{-kt} \quad (\text{Equation 9})$$

where,  $C_0$  = drug concentration at  $t = 0$  and  $k$  = the first-order release rate constant.

### Hixson-Crowell model

This model is used when the drug release is controlled by particle size reduction, and it is often applicable to tablet dissolution when the formulation involves erosion or disintegration of the dosage form over time.

$$C_0^{\frac{1}{3}} - C_t^{\frac{1}{3}} = K_{HC} t \quad (\text{Equation 10})$$

where,  $K_{HC}$  = Hixson-Crowell rate constant.

### Higuchi model

The Higuchi model assumes that the drug release is governed by Fickian diffusion. The amount of drug released is proportional to the square root of time, which is characteristic of diffusion-controlled release from a matrix system.

$$C_t = K_H t^{\frac{1}{2}} \quad (\text{Equation 11})$$

where,  $K_H$  = Higuchi rate constant.

### Korsmeyer-Peppas model

The Korsmeyer-Peppas model is often used when the drug release mechanism involves a combination of both diffusion and erosion processes.

$$\frac{C_t}{C_\infty} = K_{KP} t^n \quad (\text{Equation 12})$$

where,  $C_\infty$  = maximum drug concentration,  $K_{KP}$  = Korsmeyer-Peppas rate constant and  $n$  = release exponent.

## RESULTS

### Drug Excipient Compatibility Studies

The FTIR spectrum of SFB confirmed the presence of all the expected functional groups. No significant differences were observed in the spectra of the drug compared to the mixtures (see Figure 2), indicating the absence of interactions between the drug and excipients.

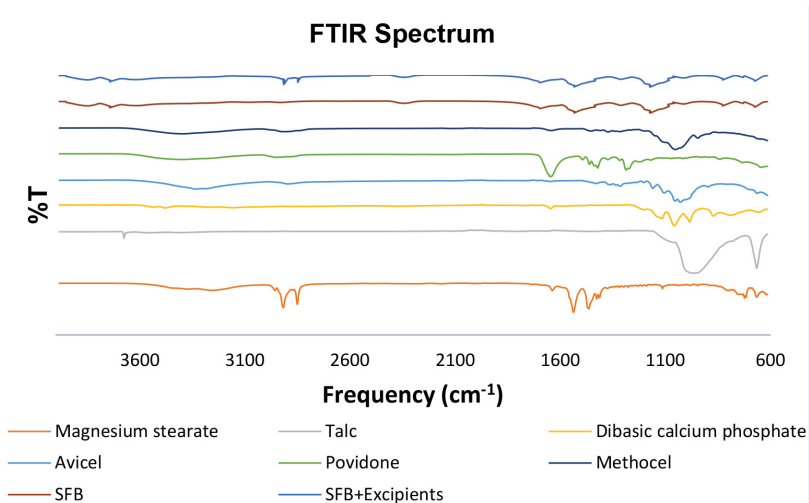


**Figure 2:** FTIR spectra of SFB, excipients and SFB/excipient mixture (1:1).

### Evaluation of Granules and Tablets

All formulations, except F3, F4 and F9, exhibited excellent flowability (see Table 4). The tablets across all batches demonstrated uniformity in size, weight, and hardness (see Table 5). The friability percentage for each batch was below 1%, indicating compliance with the specified limits.



**Table 4:** Evaluation of flow properties.

Batch	Hausner ratio	Carr's index (%)	Angle of repose (°)	Flow character
F1	1.08	8.62	28.71	Excellent
F2	1.10	9.15	29.26	Excellent
F3	1.16	12.31	33.16	Good
F4	1.14	11.37	31.48	Good
F5	1.06	7.23	27.33	Excellent
F6	1.08	8.34	28.29	Excellent
F7	1.07	7.82	27.92	Excellent
F8	1.04	6.58	26.48	Excellent
F9	1.16	12.45	33.35	Good

**Table 5:** Evaluation of physical properties of tablets.

Batch	Length ± %RSD	Width ± %RSD	Thickness ± %RSD	Average weight (mg) ± %RSD	Hardness (kg/cm <sup>2</sup> )	Friability (%)
F1	17.25±0.06	8.51±0.09	6.12±0.06	563.31±0.08	11.20	0.27
F2	17.24±0.04	8.52±0.10	6.11±0.05	575.76±0.05	11.34	0.26
F3	17.16±0.02	8.56±0.04	6.06±0.03	564.92±0.04	11.30	0.19
F4	17.21±0.05	8.53±0.06	6.10±0.04	570.67±0.06	12.01	0.32
F5	17.25±0.07	8.52±0.08	6.11±0.05	573.46±0.05	11.07	0.33
F6	17.22±0.04	8.53±0.06	6.10±0.04	566.82±0.06	12.07	0.28
F7	17.17±0.03	8.56±0.05	6.07±0.01	568.53±0.03	11.05	0.29
F8	17.18±0.05	8.55±0.05	6.08±0.02	567.72±0.07	11.09	0.34
F9	17.19±0.04	8.54±0.06	6.09±0.02	567.72±0.07	11.04	0.22

### In Vitro Dissolution Studies of F1–F9 Formulations

The dissolution profiles of the nine batches (see Table 6) showed varying release patterns. The initial release at 2 hours ranged from 6.53%–21.62%, while the release after 8 hours varied between 52.25%– 74.35%. After 12 hours, the drug release ranged from 78.13%–97.65%. These dissolution data were used for further analysis, which contributed to the development of the optimal formulation.

**Table 6:** In vitro dissolution studies of F1–F9 formulations.

Time (h)	Cumulative % of drug release								
	F1	F2	F3	F4	F5	F6	F7	F8	F9
2	16.34	10.38	13.12	10.12	19.29	13.73	18.17	21.62	6.53
8	66.76	62.87	56.34	59.34	71.46	66.27	68.43	74.35	52.25
12	88.45	84.66	81.91	83.64	92.58	85.54	91.11	97.65	78.13

## Response Surface Analysis

The analysis of variance (ANOVA) results (see Table 7) indicated that factors A and B significantly impacted responses R1, R2 and R3. The contour plots illustrated the interactions between the independent variables on response R1 (see Figures 3 and 4), response R2 (see Figures 5 and 6) and response R3 (see Figures 7 and 8). Each response model demonstrated a strong fit, with high *f*-values of 74.76, 105.68 and 74.73 for R1, R2 and R3, respectively, and *p*-values < 0.0001, confirming statistical significance. Factor A showed a particularly strong influence across all responses, with *f*-values of 122.96, 126.95 and 93.9 for R1, R2 and R3, respectively, and *p*-values < 0.0001. Factor B also significantly affected each response, especially R2 (*f* = 84.4, *p* < 0.0001) and R3 (*f* = 55.56, *p* = 0.0003).

The regression equations for each response quantified these effects, with negative coefficients indicating that increasing levels of A and B reduced response values. Model reliability was supported by fit statistics, including low standard deviations (1.11 for R1, 1.38 for R2 and 1.36 for R3) and high adequate precision (AP) values (22.89, 28.79 and 24.14), which suggested strong signal-to-noise ratios. Additionally, the coefficients of variation (C.V.) for each response were below 8%, indicating that the models predicted responses with high accuracy within the experimental design range.

**Table 7:** ANOVA summary and regression analysis for response variables.

ANOVA for the responses									
		R1		R2			R3		
Source	SS <sup>a</sup>	<i>f</i>	<i>p</i>	SS	<i>f</i>	<i>p</i>	SS	<i>f</i>	<i>p</i>
Model	185.08	74.76	< 0.0001	402.98	105.68	< 0.0001	275.91	74.73	< 0.0001
A	152.21	122.96	< 0.0001	242.06	126.95	< 0.0001	173.34	93.90	< 0.0001
B	32.87	26.56	0.0021	160.92	84.40	< 0.0001	102.57	55.56	0.0003
Residual	7.43			11.44			11.08		
Cor Total	192.51			414.42			286.99		
Fit statistics				Regression equation (Coded)					
Source	R1	R2	R3	R1 = +14.17 – 5.04A – 2.32B					
Std. Dev.	1.11	1.38	1.36	R2 = +63.80 – 6.35A – 5.13B					
Mean	14.37	64.23	87.07	R3 = +86.73 – 5.38A – 4.09B					
C.V. %	7.74	2.15	1.56						
AP <sup>b</sup>	22.8947	28.7934	24.1371						

Notes: SS<sup>a</sup> = Sum of squares; AP<sup>b</sup> = Adequate precision.

Factor Coding: Actual

Cumulative % drug release after 2 h (%)

● Design Points

6.53 21.62

X1 = A

X2 = B

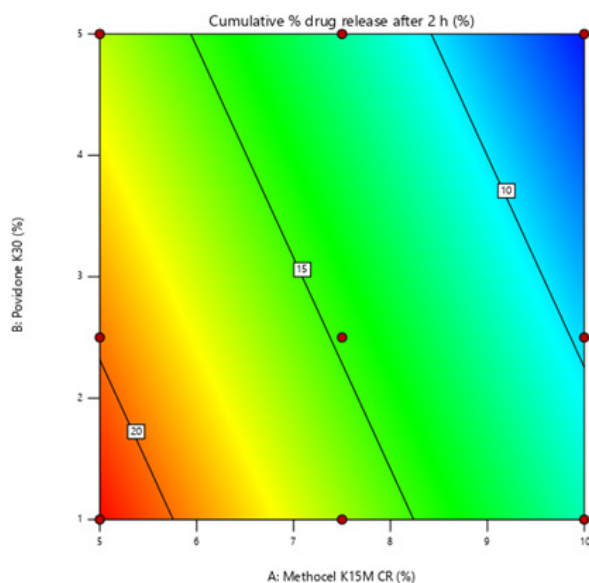


Figure 3: 2D contour plot for drug release after 2 hours.

Factor Coding: Actual

Cumulative % drug release after 2 h (%)

Design Points:

● Above Surface

○ Below Surface

6.53 21.62

X1 = A

X2 = B

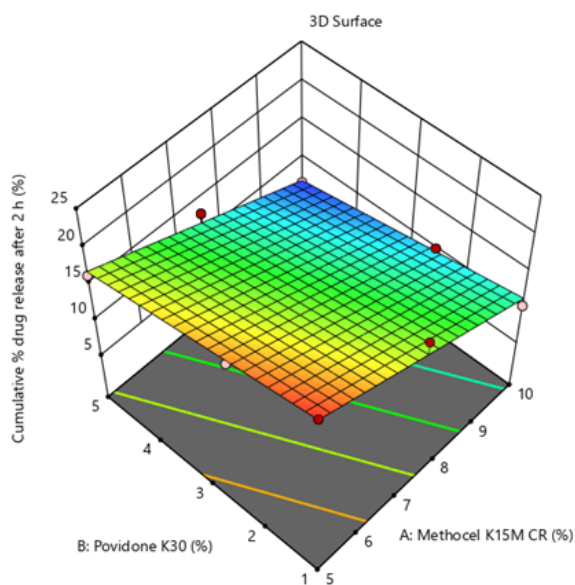


Figure 4: 3D surface response plot for drug release after 2 hours.

Factor Coding: Actual

Cumulative % drug release after 8 h (%)

● Design Points

52.25 74.35

X1 = A

X2 = B

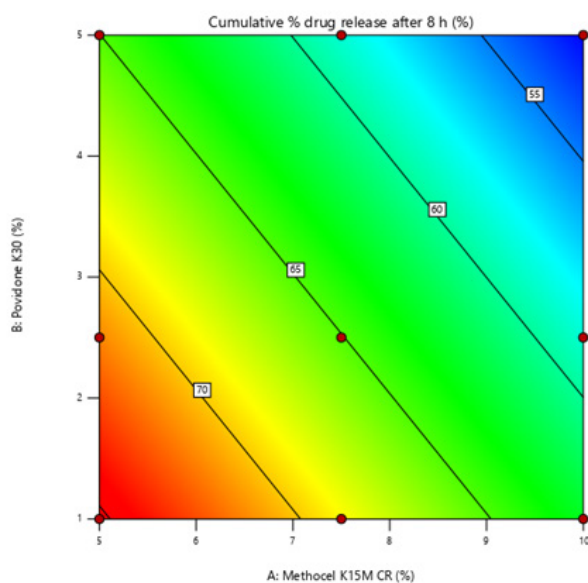


**Figure 5:** 2D contour plot for drug release after 8 hours.

Factor Coding: Actual

Cumulative % drug release after 8 h (%)

Design Points:

● Above Surface

○ Below Surface

52.25 74.35

X1 = A

X2 = B

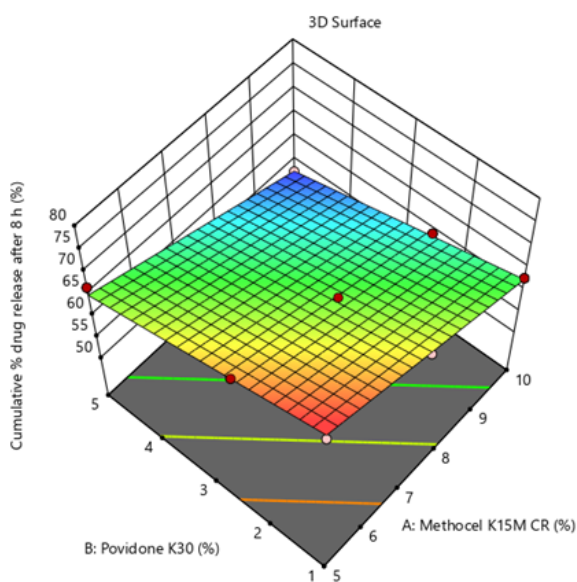


**Figure 6:** 3D surface response plot for drug release after 8 hours.

Factor Coding: Actual

Cumulative % drug release after 12 h (%)

● Design Points

78.13 97.65

X1 = A

X2 = B

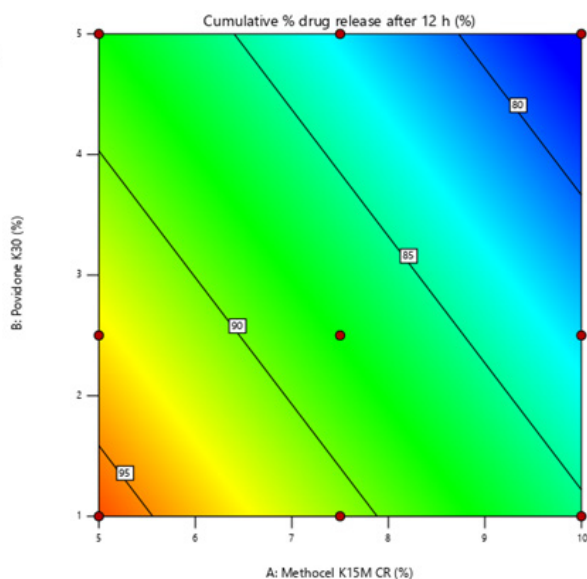


Figure 7: 2D contour plot for drug release after 12 hours.

Factor Coding: Actual

Cumulative % drug release after 12 h (%)

Design Points:

● Above Surface

○ Below Surface

78.13 97.65

X1 = A

X2 = B

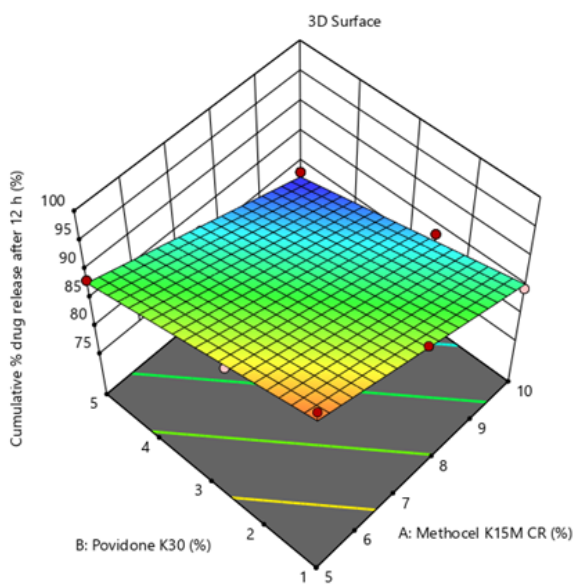


Figure 8: 3D surface response plot for drug release after 12 hours.

## Formulation Optimisation

An overlay plot (see Figure 9) was generated to evaluate the drug release models at  $Q_2$ ,  $Q_8$  and  $Q_{12}$ , helping to identify the range where both independent variables met the USP dissolution requirements. Figure 10 shows the results of the optimisation analysis, where the factors Methocel® K15M and Povidone K30 were adjusted to optimise the outcomes for three response variables (R1, R2 and R3). The optimal levels of Methocel® K15M and Povidone K30 were approximately 6.05407% and 4.38732%, respectively. These settings yielded predicted response values of 15.4797 for R1, 63.921 for R2 and 87.0037 for R3. An overall desirability score of 1.000 indicates that this combination of factor levels perfectly satisfies the criteria for all responses, representing the optimal solution out of 100 possible combinations. Table 8 displays the observed experimental values of the responses along with the percentage errors calculated from the predicted values.

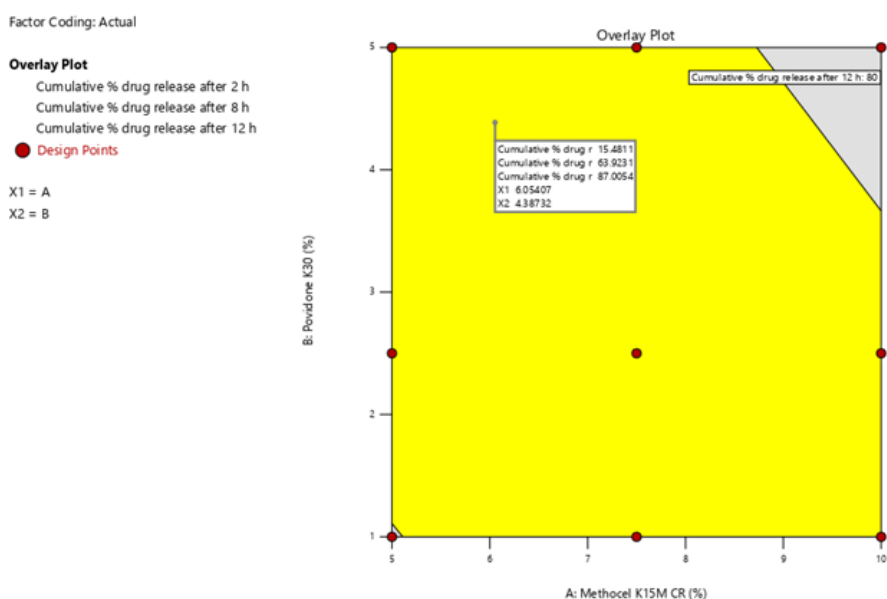
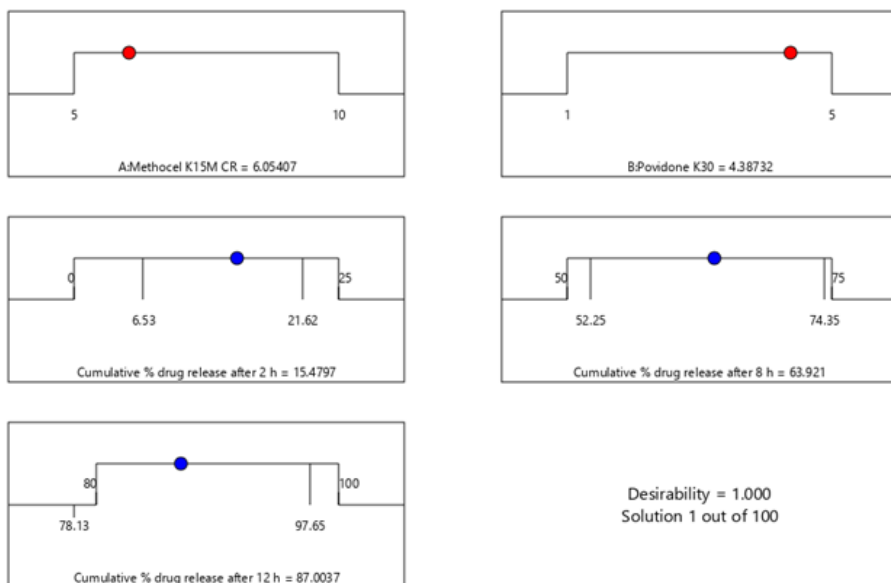


Figure 9: The overlay plot of the optimisation area.



**Figure 10:** Levels of independent variables in optimised formulation with predicted responses.

**Table 8:** Predicted and observed responses of the optimised formulation.

Responses	Predicted	Observed	Predicted error <sup>a</sup>	Remarks
Q <sub>2</sub>	15.4797	15.56	0.516%	Satisfactory
Q <sub>8</sub>	63.9210	64.33	0.636%	Satisfactory
Q <sub>12</sub>	87.0037	87.12	0.133%	Satisfactory

Notes: Predicted error<sup>a</sup> = (observed value–predicted value)/observed value × 100%; Tolerance = ± 2%

### In Vitro Drug Release Kinetics Studies

The optimised tablet batch exhibited the highest  $R^2$  value of 0.9999 in the Higuchi model. Graphs for in vitro release kinetics studies are provided in Figure 11.

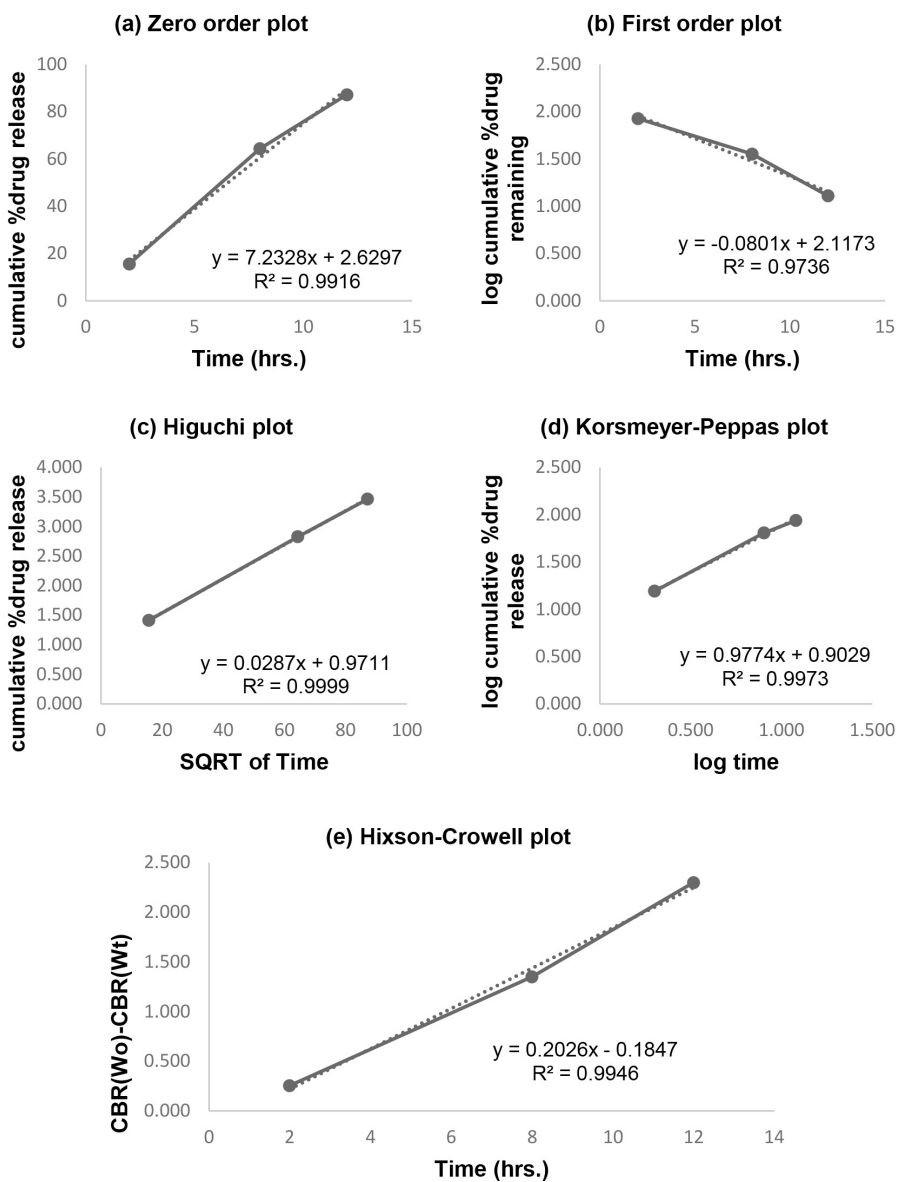


**Figure 11:** Release kinetics of the optimised batch in (a) zero order, (b) first order, (c) Higuchi, (d) Korsmeyer-Peppas and (e) Hixson-Crowell plots.



## DISCUSSION

This study contrasts with previous research on SFB formulations by specifically focusing on developing a sustained release hydrophilic matrix tablet using factorial design to optimise drug release over an extended period. Kane *et al.* (2006) documented the initial FDA approval of SFB tosylate 200 mg tablets, formulated as immediate release tablets for advanced renal cell carcinoma. Their formulation used disintegrants and fillers like croscarmellose sodium and microcrystalline cellulose without targeting a prolonged release profile (Kane *et al.* 2006). In comparison, the present study aimed to enhance patient compliance by designing a 400 mg sustained release tablet using HPMC as a matrix forming agent. This approach allows steady drug release over 12 hours.

In the study by Park *et al.* (2019), the researchers applied a nanoparticulation technique to improve SFB's bioavailability by reducing particle size and using HPMC and polyvinyl pyrrolidone K30 (PVP) to stabilise the nanoparticles (Park *et al.* 2019). Whereas Park's study focused on enhancing drug absorption using nanoparticles, this study employed a hydrophilic matrix system to optimise sustained release via factorial design rather than through particle size modification or encapsulation. The matrix-based design in this study is intended to simplify dosing schedule rather than maximising immediate absorption, as seen with nanoparticulate formulations.

Reddy and Kalpana (2020) developed immediate release SFB tosylate tablets through a direct compression method, incorporating superdisintegrants like Explotab and Solutab to achieve rapid drug release. Their design resulted in drug dissolution within 45 minutes, in contrast to the sustained release profile in this study, which was designed for gradual drug release over a 12 hour period (Reddy and Kalpana 2020). Thus, while Reddy and Kalpana's approach prioritises immediate bioavailability, this study's sustained-release tablet potentially offers more consistent therapeutic plasma levels, improving patient adherence with reduced number of tablet intake.

The study by Kenjale and Pokharkar (2022) used a quality by design framework to create a SFB tosylate colon-targeted bilayer tablet, optimising disintegration and drug release for localised delivery in the colon (Kenjale and Pokharkar 2022). In contrast, the present study focused on achieving systemic sustained release rather than localised colonic delivery. By selecting a factorial design approach, the current study enabled controlled optimisation of HPMC and Povidone K30 levels to meet systemic therapeutic needs, differing from the localised approach in Kenjale and Pokharkar's formulation.

Finally, Mans and Dong (2023) formulated lipid-based SFB granules to improve SFB's solubility and bioavailability in gastric and intestinal fluids. Their lipid-coating technique enhanced immediate release in these fluids (Mans and Dong 2023). By contrast, the hydrophilic matrix system in this study achieves a sustained release profile, focusing on dosing convenience rather than rapid absorption.

Overall, this study contributes a unique sustained-release formulation to the existing range of SFB delivery systems, focusing on simplifying dosing regimens and achieving a stable release profile. Unlike previous studies, which either aimed at immediate release for rapid absorption, bioavailability enhancement, or targeted release for specific regions in the digestive tract, this sustained release tablet approach may provide a viable alternative for patients who require consistent SFB plasma levels with improved adherence to a simplified dosing regimen.

## CONCLUSION

A novel sustained release formulation of SFB was successfully developed using a combination of excipients. The formulation was optimised through a 3<sup>2</sup> full factorial design in Design Expert® software, enabling a systematic assessment of various factors and their interactions. This QbD approach facilitated the development of an optimised formulation with ideal drug release characteristics. The results underscored the importance of carefully selecting appropriate excipients and optimising their concentrations to achieve the desired drug release profile.

## ACKNOWLEDGEMENTS

The authors extend their gratitude to Eskayef Pharmaceuticals Limited, Bangladesh, for supplying the reference standard of sorafenib and essential excipients. Appreciation is also given to the technical staff of the Department of Pharmacy, East West University for their valuable support throughout the research process.

## REFERENCES

- ABDU, S., JUAID, N., AMIN, A., MOULAY, M. *et al.* (2022) Effects of sorafenib and quercetin alone or in combination in treating hepatocellular carcinoma: In vitro and in vivo approaches, *Molecules*, 27(22): 8082. <https://doi.org/10.3390/molecules27228082>
- ALGHAMDI, M. A., AMARO, C. P., LEE-YING, R., SIM, H. W. *et al.* (2020) Effect of sorafenib starting dose and dose intensity on survival in patients with hepatocellular carcinoma: Results from a Canadian multicenter database, *Cancer Medicine*, 9(14): 4918–4928. <https://doi.org/10.1002/cam4.3228>
- AMAN, A., ALI, S., MAHALAPBUTR, P., KRUSONG, K. *et al.* (2023) Enhancing solubility and stability of sorafenib through cyclodextrin-based inclusion complexation: In silico and in vitro studies, *RSC Advances*, 13(39): 27244–27254. <https://doi.org/10.1039/D3RA03867J>
- CHAUDHARI, A.R., GUJARATHI, N.A., RANE, B.R., PAWAR, S.P. & BAKLIWAL, S. P. (2012) Novel sustained release drug delivery system: A review, *Pharma Research*, 8(1): 80–97.
- CHENG, A. L., QIN, S., IKEDA, M., GALLE, P. R. *et al.* (2022) Updated efficacy and safety data from IMbrave150: Atezolizumab plus bevacizumab vs. sorafenib for unresectable hepatocellular carcinoma, *Journal of Hepatology*, 76(4): 862–873. <https://doi.org/10.1016/j.jhep.2021.11.030>
- DARANDALE, A. S., GHULE, P. J., AHER, A. A. & NARWATE, B. M. (2017) Sustained release dosage form: A concise review, *International Journal of Pharmaceutics and Drug Analysis*, 5(5): 153–160.
- GOLDFARB, H. B. (2006) Experimental design for formulation, *Technometrics*, 48(2): 304–304. <https://doi.org/10.1198/tech.2006.s380>

GOYAL, S., AGARWAL, G., AGARWAL, S. & KARAR, P. K. (2017) Oral sustained release tablets: An overview with a special emphasis on matrix tablet, *American Journal of Advanced Drug Delivery*, 5(4): 1–13. <https://doi.org/10.21767/2321-547X.1000013>

HWANG, R. & NOACK, R. M. (2011) Application of design of experiments to pharmaceutical formulation development, *International Journal of Experimental Design and Process Optimisation*, 2(1): 58. <https://doi.org/10.1504/IJEDPO.2011.038051>

KAMBOJ, S., SAROHA, K., GOEL, M. & MADHU, C. (2012) Sustained release drug delivery system: An overview, *Pharma Research*, 8(1): 169–186.

KANE, R. C., FARRELL, A. T., SABER, H., TANG, S. *et al.* (2006) Sorafenib for the treatment of advanced renal cell carcinoma, *Clinical Cancer Research*, 12(24): 7271–7278. <https://doi.org/10.1158/1078-0432.CCR-06-1249>

KENJALE, P. & POKHARKAR, V. (2022) Risk assessment and QbD-based optimization of sorafenib tosylate colon targeted bilayer tablet: in vitro characterization, in vivo pharmacokinetic, and in vivo roentgenography studies, *AAPS PharmSciTech*, 23(6): 1–15. <https://doi.org/10.1208/s12249-022-02340-7>

KOLEKAR, Y. M. (2019) Understanding of DoE and its advantages in pharmaceutical development as per QbD approach, *Asian Journal of Pharmacy and Technology*, 9(4): 271–275. <https://doi.org/10.5958/2231-5713.2019.00045.X>

KONG, F. H., YE, Q. F., MIAO, X. Y., LIU, X. *et al.* (2021) Current status of sorafenib nanoparticle delivery systems in the treatment of hepatocellular carcinoma, *Theranostics*, 11(11): 5464–5490. <https://doi.org/10.7150/thno.54822>

KOVÁCS, B., PÉTERFI, O., KOVÁCS-DEÁK, B., SZÉKELY-SZENTMIKLÓSI, I. *et al.* (2021) Quality-by-design in pharmaceutical development: from current perspectives to practical applications, *Acta Pharmaceutica*, 71(4): 497–526. <https://doi.org/10.2478/acph-2021-0039>

LI, Y., YANG, W., ZHENG, Y., DAI, W. *et al.* (2023) Targeting fatty acid synthase modulates sensitivity of hepatocellular carcinoma to sorafenib via ferroptosis, *Journal of Experimental and Clinical Cancer Research*, 42(1): 1–19. <https://doi.org/10.1186/s13046-022-02567-z>

LLOVET, J. M., RICCI, S., MAZZAFERRO, V., HILGARD, P. *et al.* (2008) Sorafenib in advanced hepatocellular carcinoma, *New England Journal of Medicine*, 359(4): 378–390. <https://doi.org/10.1056/NEJMoa0708857>

MAMIDALA, R. K., RAMANA, V., SANDEEP, G., LINGAM, M. *et al.* (2009) Factors influencing the design and performance of oral sustained/controlled release dosage forms, *International Journal of Pharmaceutical Sciences and Nanotechnology*, 2(3): 583–594. <https://doi.org/10.37285/ijpsn.2009.2.3.1>

MAN, S., LUO, C., YAN, M., ZHAO, G. *et al.* (2021) Treatment for liver cancer: From sorafenib to natural products, *European Journal of Medicinal Chemistry*, 224: 113690. <https://doi.org/10.1016/j.ejmech.2021.113690>

MANS, J. C. & DONG, X. (2023) The development of lipid-based sorafenib granules to enhance the oral absorption of sorafenib, *Pharmaceutics*, 15(12): 2691. <https://doi.org/10.3390/pharmaceutics15122691>

NANDI, T., KUMAR, U., BHADRA, S. & ROUF, A. S. S. (2022) Formulation design and optimization of hydrophilic matrix based sustained release tablet of clarithromycin using a design of experiment (DoE), *Journal of Advances in Medicine and Medical Research*, 34(24): 274–287. <https://doi.org/10.9734/jammr/2022/v34i244926>

PANG, Y., ERESEN, A., ZHANG, Z., HOU, Q. et al. (2022) Adverse events of sorafenib in hepatocellular carcinoma treatment, *American Journal of Cancer Research*, 12(6): 2770–2782.

PARK, S. Y., KANG, Z., THAPA, P., JIN, Y. S. et al. (2019) Development of sorafenib loaded nanoparticles to improve oral bioavailability using a quality by design approach, *International Journal of Pharmaceutics*, 566: 229–238. <https://doi.org/10.1016/j.ijpharm.2019.05.064>

POLITIS, S. N., COLOMBO, P., COLOMBO, G. & REKKAS, D. M. (2017) Design of experiments (DoE) in pharmaceutical development, *Drug Development and Industrial Pharmacy*, 43(6): 889–901. <https://doi.org/10.1080/03639045.2017.1291672>

PUNDIR, S., BADOLA, A. & SHARMA, D. (2013) Sustained release matrix technology and recent advance in matrix drug delivery system: A review, *International Journal of Drug Research and Technology*, 3(1): 12–20.

REDDY, Y. K. & KALPANA, D. (2020) Formulation development and evaluation of immediate release tablet dosage form of sorafenib tosylate, *Asian Journal of Pharmacy and Technology*, 10(1): 38–42. <https://doi.org/10.5958/2231-5713.2020.00008.2>

TAK, K. Y., NAM, H. C., CHOI, J. Y., YOON, S. K. et al. (2020) Effectiveness of sorafenib dose modifications on treatment outcome of hepatocellular carcinoma: Analysis in real-life settings, *International Journal of Cancer*, 147(7): 1970–1978.

TANG, W., CHEN, Z., ZHANG, W., CHENG, Y. et al. (2020) The mechanisms of sorafenib resistance in hepatocellular carcinoma: theoretical basis and therapeutic aspects, *Signal Transduction and Targeted Therapy*, 5(1): 1–15. <https://doi.org/10.1038/s41392-020-0187-x>

WU, F. & JIN, T. (2008) Polymer-based sustained-release dosage forms for protein drugs, challenges, and recent advances, *AAPS PharmSciTech*, 9(4): 1218–1229. <https://doi.org/10.1208/s12249-008-9148-3>

YU, L. X., AMIDON, G., KHAN, M. A., HOAG, S. W. et al. (2014) Understanding pharmaceutical quality by design, *AAPS Journal*, 16(4): 771–783. <https://doi.org/10.1208/s12248-014-9598-3>